Drug Design

Deutsche Ausgabe: DOI: 10.1002/ange.201607474
Internationale Ausgabe: DOI: 10.1002/anie.201607474

Improvement of Ligand Affinity and Thermodynamic Properties by NMR-Based Evaluation of Local Dynamics and Surface Complementarity in the Receptor-Bound State

*Yumiko Mizukoshi[+], Koh Takeuchi[+], Misa Arutaki, Yuji Tokunaga, Takeshi Takizawa, Hiroyuki Hanzawa, and Ichio Shimada**

Abstract: *The thermodynamic properties of a ligand in the bound state affect its binding specificity. Strict binding specificity can be achieved by introducing multiple spatially defined interactions, such as hydrogen bonds and van der Waals interactions, into the ligand–receptor interface. These introduced interactions are characterized by restricted local dynamics and improved surface complementarity in the bound state. In this study, we experimentally evaluated the local dynamics and the surface complementarity of weak-affinity ligands in the receptor-bound state by forbidden coherence transfer analysis in free-bound exchange systems (Ex-FCT), using the interaction between a ligand, a myocyte-enhancer factor 2A (MEF2A) docking peptide, and a receptor, p38α, as a model system. The Ex-FCT analyses successfully provided information for the rational design of a ligand with higher affinity and preferable thermodynamic properties for p38α.*

Weak-affinity ligands in the initial stage of a drug discovery are subjected to a hit-to-lead process, in which the affinity and specificity of the ligands are improved by modification of their structure. Structure-guided drug development (SGDD) is one of the major strategies utilized in this process and various methods using X-ray crystallography, solution NMR, and in silico molecular modeling have been proposed.[1] In addition to structural methods, the thermodynamic properties of ligand–receptor interactions have recently attracted attention due to their connection to the binding specificity and the adaptability to drug-resistant mutations in the receptors.[2] Ligands with better binding specificity tend to have more enthalpic interactions,[2,3] and those ligands that have high enthalpic contributions in their binding free energy can counter drug-resistant mutations in the receptors.[4] Enthalpic interactions are achieved by the formation of spatially defined interactions, such as hydrogen bonds and van der Waals interactions, in the ligand–receptor interfaces. However, the design of ligands with better thermodynamic properties is currently difficult.

The introduction of enthalpic interactions to the ligand–receptor interfaces is reflected by the restricted local dynamics and the improved surface complementarity in the bound state.[4,5] Solution NMR is a suitable technique for the quantitative monitoring of those metrics in the ligand–receptor interactions.[6]

In addition to those strategies, the forbidden coherence transfer (FCT) method has been proposed, to estimate the pico- to nanosecond dynamics of methyl groups.[7] In a FCT experiment, the intensity of the multi quantum methyl proton signal (I_{mqc}) relative to the intensity of the corresponding single quantum methyl proton signal (I_{1qc}) is measured. The evolution of I_{mqc}/I_{1qc} at the time point T can be described by a formula that includes parameters η_b and δ_b, which are directly correlated with the methyl order parameter (S^2) and the dipole cross-correlated relaxation rate to external protons, respectively (details are given in the experimental section in the Supporting Information, Figure S1).[7b] As shown in Figure S1, the slope of the I_{3qc}/I_{1qc} build-up curve depends on the value of S^2. Therefore, the local dynamics of the ligand methyl groups in the ligand–receptor complex can be obtained by the FCT method.

Furthermore, an acceptable correlation reportedly exists between the δ_b values calculated from the FCT experiments and the X-ray coordinates.[7b,8] Methyl groups with external protons in their vicinity have large negative δ_b values, which are reflected in the lower plateau values in the I_{mqc}/I_{1qc} build-up (Figure S1b). The contribution of external protons to the δ_b values is substantial when $r_{eff} = (\Sigma_{ext} r_{ext,HH}^{-6})^6 < 3.0$ Å,[8] while the effects are only marginal when r_{eff} is > 4.0 Å (Figure S1c). A 3.0 Å distance is almost comparable to the size of methyl (2.9 Å) and halogen (2.2–4.2 Å) substituents; therefore, the FCT experiment is sensitive to the degree of surface complementarity of each methyl group at the ligand–receptor interface. Although these features have not been experimentally explored thus far, here we propose that changing the proton density of the receptor by fractional

[*] Prof. Dr. I. Shimada
Graduate School of Pharmaceutical Sciences, The University of Tokyo
Hongo 7-3-1, Bunkyo-ku, Tokyo 113-0033 (Japan)
E-mail: shimada@iw-nmr.f.u-tokyo.ac.jp
Dr. Y. Mizukoshi,[+] Dr. K. Takeuchi,[+] M. Arutaki, Dr. Y. Tokunaga, Prof. Dr. I. Shimada
Biomedicinal Information Research Center (BIRC) and Molecular Profiling Research Center (Molprof), National Institute of Advanced Industrial Science and Technology (AIST)
2-3-26 Aomi, Koto-ku, Tokyo 135-0064 (Japan)
Dr. Y. Mizukoshi,[+] M. Arutaki, Dr. Y. Tokunaga
Japan Biological Informatics Consortium (JBIC)
2-3-26 Aomi, Koto-ku, Tokyo 135-0064 (Japan)
T. Takizawa, Dr. H. Hanzawa
Structural Biology Group, Biological Research Department
Daiichi Sankyo RD Novare Co. LTD.
1-16-13 Kitakasai, Edogawa-ku, Tokyo 134-8630 (Japan)
[+] These authors contributed equally to this work.
Supporting information for this article can be found under: http://dx.doi.org/10.1002/anie.201607474.

deuteration would affect the δ_b values of the bound ligand, and the difference of the δ_b values ($\Delta\delta_b$) between the perdeuterated and fractionally deuterated conditions would be more substantial for methyl groups that are buried deeply in the receptor with optimal surface complementarity to the receptor.

Therefore, FCT experiments are suitable for the rational design of better ligands with restricted local dynamics and improved surface complementarity in the receptor-bound state. The applicability of the FCT method to high molecular-weight (M_w) proteins is attractive for SGDD, because the proteins of interest in drug discovery tend to be large ($M_w >$ 40 K). While the current FCT experiment is applicable to a ligand in the fully bound state, its application to weak-affinity ligands that exhibit free-bound exchange in solution is not straightforward.

In this study, we have theoretically extended the FCT method to the systems under free-bound exchange (Ex-FCT), to evaluate the local dynamics and the surface complementarity of weak-affinity ligands in the receptor-bound state. By applying the Ex-FCT method to the interaction between the ligand, myocyte-enhancer factor 2A (MEF2A) docking peptide (Figure S2a, M_w: 1.6 K), and the receptor, mitogen-activated protein kinase p38α (M_w: 42 K),[9] the dynamics of the ligand methyl groups in the receptor-bound state were quantitatively estimated in exchanging conditions, where the ligand is present in excess relative to the receptor. The surface complementarity around the ligand methyl groups was also analyzed by using the Ex-FCT method, with the proton density of the receptor varied by fractional deuteration. Based on these Ex-FCT derived information, we introduced a rational mutation to the MEF2A docking peptide and were able to obtain a ligand with higher receptor affinity and better thermodynamic properties than those of the original ligand.

In a system with fast exchange between the free and bound states, the reported equations for the FCT experiment [Eqs. (S4)–(S6)][7b] can be extended as follows with the bound ratio (p_b).

$$I_{3qc}/I_{1qc} = \frac{-0.75\eta_{ex}\tanh\left(\sqrt{\eta_{ex}^2+\delta_{ex}^2}T\right)}{\sqrt{\eta_{ex}^2+\delta_{ex}^2}-\delta_{ex}\tanh\left(\sqrt{\eta_{ex}^2+\delta_{ex}^2}T\right)} \quad (1)$$

$$\eta_{ex} = p_b\eta_b + (1-p_b)\eta_f \quad (2)$$

$$\delta_{ex} = p_b\delta_b + (1-p_b)\delta_f \quad (3)$$

where η_{ex} and δ_{ex} are the population averages of η and δ in the free and bound states, respectively. As shown in the simulated build-up curves, the slope of the curve largely depends on p_b and η_b (Figures 1a and S1d, respectively). Therefore, from two separate experiments with distinct p_b values, η_b and δ_b for each methyl in the bound state can be determined, along with η_f and δ_f values. Furthermore, since the magnitudes of the η and δ values are proportional to the M_w of the system, the contribution of the bound state coherences to the Ex-FCT profile is expected to be more substantial than that of the free state. Therefore, even in the Ex-FCT profile would effectively reflect the methyl dynamics in the bound state (Figure S1d). It should be noted that S^2 in the free state cannot be deduced from η_f, as its τ_c values are comparable to the methyl 3-fold

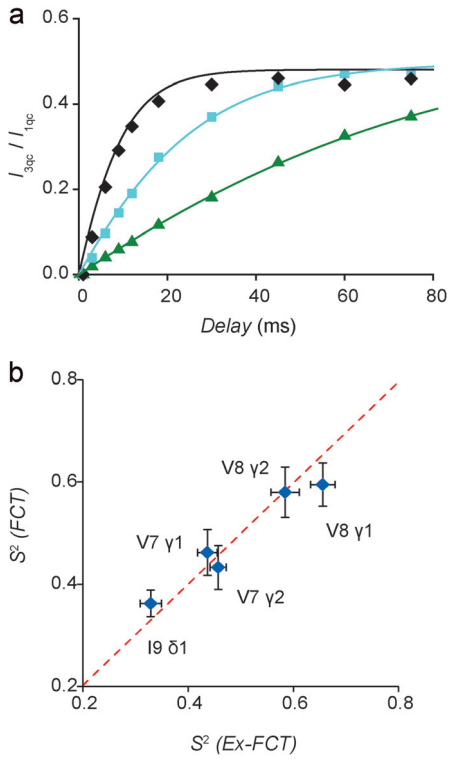

Figure 1. Analysis of the ligand methyl dynamics by the Ex-FCT experiments. a) Superimposed simulation curves of the Ex-FCT build-up on the experimental results (FCT; black diamonds, Ex-FCT $p_b = 0.35$; cyan squares, Ex-FCT $p_b = 0.08$; green triangles). The Ex-FCT build-up curves were calculated according to the Equations (S4) and (1), with η_b, η_f, δ_b, and δ_f values of 63, 4.5, −29, and −0.66, respectively, which are equal to the experimentally determined value. b) Correlation of the S^2 values determined by the Ex-FCT and FCT experiments.

axis dynamics.[10] In addition, since the proton density of the surrounding receptor surface would affect the Ex-FCT profile only through the bound state (Figure S1e), the surface complementarity for each methyl in the ligand–receptor interface can be estimated from the changes in δ_b ($\Delta\delta_b$) from a set of Ex-FCT experiments with different deuteration rates in the receptor.

For experimental verification, we chose an interaction between the MEF2A docking peptide and p38α.[9a] The crystal structure of the MEF2A docking peptide–p38α complex is available (Figure S2b, PDB ID: 1LEW)[9b,11] and the interaction is suitable for the FCT analyses, since the MEF2A docking peptide has multiple methyl-bearing residues at the ligand–receptor interface. The affinity between the MEF2A docking peptide and wild-type (WT) p38α was relatively high ($K_d = 7.4 \pm 1.0$ μM), and the chemical shift perturbations (CSPs) of the ^1H–^{13}C methyl signals of the [U-^2H, ILV-methyl-$^1H^{13}C$]-labeled MEF2A docking peptide upon the titration of WT p38α occurred on a slow to intermediate timescale. Therefore, we utilized the C119S/C162S double-mutant of p38α (p38α^{DCS}) for the Ex-FCT experiment, which is assumed to have a lower affinity for the MEF2A docking peptide but an almost identical binding conformation.[9b,11a,12] Indeed, the p38α^{DCS} mutant had a $K_d = 251 \pm 22$ μM, and thus is suitable to model the free-bound exchange of weak-affinity ligands. The CSPs of the MEF2A docking peptide upon the

titration of p38α^{DCS} showed fast exchange characteristics (Figures S2c, S2d). The methyl signals migrate toward the positions of the MEF2A docking peptide bound to WT p38α (Figures S2c–e), therefore, the conformation of the MEF2A docking peptide in complex with p38α^{DCS} is almost identical to that in complex with WT p38α.

In this study, we analyzed the local dynamics and the surface complementarity of the Val-7 γ, Val-8 γ, and Ile-9 δ1 methyl groups in the MEF2A docking peptide, which correspond to the critical Φ_A–X–Φ_B motif in the consensus docking (R/K)$_2$–X$_{2\text{-}6}$–Φ_A–X–Φ_B sequence.[9b,11a] The Ex-FCT build-up curves of Val-8 γ1 of the [U-^{2}H, ILV-methyl-^{1}H^{13}C]-labeled MEF2A docking peptide in complex with sub-stoichiometric amounts of perdeuterated p38α^{DCS} are shown in Figure 1a (Profiles for 35% and 8% bound conditions are shown in cyan and green, respectively). The FCT build-up curve from the MEF2A docking peptide in complex with the WT p38α is also shown (Figure 1a, black). The dependence of the Ex-FCT build-up curve on the bound population is consistent with a theoretical simulation (Figure 1a, solid lines), and the S^2 values of the Val-7 γ, Val-8 γ, and Ile-9 δ1 methyl groups in the bound state were successfully determined by the simultaneous fitting of the Ex-FCT build-up curves under the 35% and 8% bound conditions (Figure S3, Tables S1, S2). The S^2 values suggested that the Val-7 γ, and Ile-9 δ1 methyl groups are more dynamic, as compared to Val-8 γ, in the bound state. The S^2 value of each methyl group in the bound state, determined by the Ex-FCT experiment, was in good agreement with that obtained from the FCT experiment (Figure 1b).

Interestingly, Val-8 γ, which is more exposed to the solvent, was less dynamic as compared to Val-7 γ and Ile-9 δ1, which are located in the binding pocket of p38α. The higher S^2 values for Val-8 γ seemed to originate from the limited rotameric states of the methyl groups due to a proximal water, involved in an indirect hydrogen bond between p38α and the MEF2A docking peptide.[9b] In addition, the results also indicated that the dynamics of the methyl groups and the degrees of the surface exposure are not correlated with each other. Indeed, some methyl groups are reportedly highly dynamic in ligand–receptor interfaces, even for those of anchor residues that are essential for complex formation.[13]

In order to evaluate the surface complementarity around each methyl group in the ligand–receptor interface, a series of experiments was performed with the same free-bound ratios but with reduced deuteration rates of p38α^{DCS} (Figure S4). The change in the δ_b value in the bound state ($\Delta\delta_b$) was distinct for each methyl, reflecting the surrounding receptor (p38α^{DCS}) proton density (Table S3). The Val-7 γ1 and Ile-9 δ1 methyl groups had large negative $\Delta\delta_b$ values, while the $\Delta\delta_b$ values for Val-8 γ were almost zero (Figure 2a). Interestingly, the $\Delta\delta_b$ of Val-7 γ2 was substantial, but smaller in magnitude than those of Val-7 γ1 and Ile-9 δ1 (Figure 2a).

With 80% deuteration, the $\Delta\delta_b$ value for each methyl group showed a linear correlation with the Σr^{-6} values calculated from the X-ray structure of the MEF2A docking peptide–p38α complex (Figures 2a and 2b; PDB ID: 1LEW). The methyl groups buried deep in the pocket showed large negative $\Delta\delta_b$ values (Val-7 γ1 and Ile-9 δ1) (Figure 2b). In

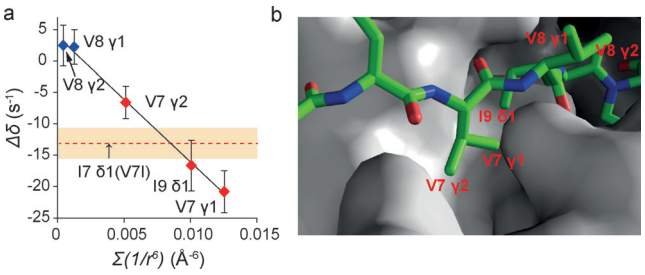

Figure 2. Analysis of the surface complementarity in the ligand–protein interface, determined by Ex-FCT experiments. a) Correlation between the $\Delta\delta_b$ values in the Ex-FCT experiment and the Σr^{-6} between the methyl and protein protons, calculated from the structure of the MEF2A docking peptide–p38α complex (PDB ID: 1LEW). The protons of p38α within 6 Å from each methyl were considered. The error bars represent fitting errors. The positive values of $\Delta\delta_b$ are within the fitting error. The red dotted line and the pale red area indicate the $\Delta\delta_b$ value and the fitting error of Ile-7 δ1 in the V7I mutant, respectively. The methyl groups with less than 10% surface exposure rates are classified as buried (red), and the rest are colored blue. b) The structure of the MEF2A docking peptide (sticks) in complex with p38α (PDB ID: 1LEW).

contrast, the Val-8 γ methyl groups that showed the smallest magnitude in $\Delta\delta_b$ values are exposed to the solvent (Figure 2b). The Val-7 γ2 methyl group with the intermediate $\Delta\delta_b$ value is buried and faces p38α in the crystal structure; however, its surface complementarity in the p38α interface is not optimal and there is extra space between the Val-7 γ2 methyl and the receptor surface (Figure 2b).

The $\Delta\delta_b$ values were more substantial with the non-deuterated p38α^{DCS} (Figure S5, Table S4). However, under the non-deuterated conditions, the linear correlation between the $\Delta\delta_b$ value for each methyl group and the calculated Σr^{-6} value from the X-ray structure becomes poorer (Figure S5), indicating that the assumption for the simplification in the determination of the δ_b values is no longer valid.[8] To avoid this problem, the reduction of the deuteration rate should be minimal.

Based on the observations derived from the Ex-FCT experiments, there is extra space around the Val-7 γ2 methyl group at the MEF2A-p38α interface. Therefore, we substituted Val-7 with larger amino acids, Phe and Ile, to see if the affinity for p38α would improve. Although the affinity of the V7F mutant for p38α decreased to $K_d = 16 \pm 2$ μM, the V7I mutant showed 3.1-fold greater affinity ($K_d = 2.4 \pm 0.2$ μM) than that of the WT MEF2A docking peptide ($K_d = 7.4 \pm 1.0$ μM) for the WT p38α. Given the sizes of phenyl (≈ 6 Å) and methyl (≈ 3 Å) groups and the r_{eff} that affects the FCT profile (< 3 Å, Figure S1c), the phenyl group is too large to be incorporated, while the smaller modification is suitable to fill the lack of surface complementarity detected by the Ex-FCT analyses. It should be noted that the incorporation of methyl groups is a common strategy to improve the activity of small molecules,[14] and thus the information obtained from the Ex-FCT experiments can be used to find the suitable sites for this modification.

The dynamics and the surface complementarity of the high-affinity V7I mutant in the interface of p38α were evaluated by the FCT/Ex-FCT experiments. The dynamic

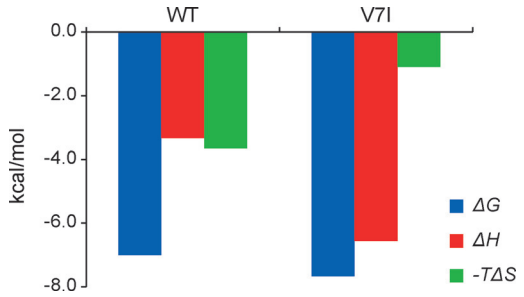

Figure 3. Binding thermodynamics of the WT MEF2A docking peptide and the V7I mutant. Calorimetric titrations of p38α with the WT MEF docking peptide or the V7I mutant were performed.

properties of the V7I mutant were mostly equivalent to those of the WT MEF2A docking peptide (Figures S6a, S6b and Table S5). In contrast, the extended Ile-7 δ1 methyl in the V7I mutant showed substantially better surface complementarity than that of the original Val-7 γ2 methyl group, as indicated by the large negative $\Delta\delta_b$ value upon the reduction of the $p38\alpha^{DCS}$ deuteration rate to 80% (Figure S7, Table S6). Isothermal titration calorimetry (ITC) experiments with the WT and V7I mutant MEF2A docking peptides with WT p38α indicated that the thermodynamic parameters of the V7I mutant were substantially improved, with higher enthalpic contributions to the binding free energy (Figure 3). These results are consistent with the improved surface complementarity at the ligand–receptor interface. The ITC experiments performed with other buffers further confirmed that the changes in the thermodynamic parameters are due to the optimization of the surface complementarity and are not due to the differences in the proton ionization effect (Figure S8).[15] The enthalpy–entropy compensation is clearly present, however a 3-fold improvement in affinity was achieved (Figure 3).[2,16]

Therefore, the dynamics and the surface complementarity information obtained from the Ex-FCT experiments will facilitate the design of ligands with improved affinities and preferable thermodynamic properties.

In the Ex-FCT experiments performed here, we used 11 different time points to obtain the FCT build-up. However, the reduction of the number of the points to half did not affect the estimation of the local dynamics and the surface complementarity (Figure S9). Therefore, the Ex-FCT experiments would be applicable to proteins that are unstable under experimental conditions, and the improved throughput is also beneficial for handling a large set of early stage hit compounds.

The comparison between the different methyl groups in a ligand enables us to predict the position(s) that should be optimized, without knowing the atomic-resolution structure of the ligand–receptor complex. In addition, the information from the Ex-FCT method can be used to build a rational model of the ligand–receptor complex. Above all, a ligand that is fine-tuned by this method can concomitantly achieve strict specificity for its receptor and robust mutant adaptability. Therefore, our proposed Ex-FCT method is beneficial for SGDD.

Acknowledgements

This work was supported by grants from the Ministry of Economy, Trade and Industry (METI).

Keywords: drug design · ligand–receptor interface · NMR spectroscopy · structural biology · surface complementarity

How to cite: *Angew. Chem. Int. Ed.* **2016**, *55*, 14606–14609
Angew. Chem. **2016**, *128*, 14826–14829

[1] a) T. L. Blundell, H. Jhoti, C. Abell, *Nat. Rev. Drug Discovery* **2002**, *1*, 45–54; b) G. E. de Kloe, D. Bailey, R. Leurs, I. J. P. de Esch, *Drug Discovery Today* **2009**, *14*, 630–646.
[2] G. Klebe, *Nat. Rev. Drug Discovery* **2015**, *14*, 95–110.
[3] a) Á. Tarcsay, G. M. Keserű, *Drug Discovery Today* **2015**, *20*, 86–94; b) A. Ali, R. M. Bandaranayake, Y. Cai, N. M. King, M. Kolli, S. Mittal, J. F. Murzycki, M. N. L. Nalam, E. A. Nalivaika, A. Özen, M. M. Prabu-Jeyabalan, K. Thayer, C. A. Schiffer, *Viruses* **2010**, *2*, 2509.
[4] H. Ohtaka, A. Schön, E. Freire, *Biochemistry* **2003**, *42*, 13659–13666.
[5] A. J. Wand, *Nat. Struct. Mol. Biol.* **2001**, *8*, 926–931.
[6] a) M. Akke, *Biochem. Soc. Trans.* **2012**, *40*, 419–423; b) G. Lipari, A. Szabo, *J. Am. Chem. Soc.* **1982**, *104*, 4546–4559; c) M. A. Markus, K. T. Dayie, P. Matsudaira, G. Wagner, *Biochemistry* **1996**, *35*, 1722–1732; d) A. G. Palmer, C. D. Kroenke, J. Patrick Loria, *Methods Enzymol.* **2001**, *339*, 204–238; e) F. Massi, M. J. Grey, A. G. Palmer, *Protein Sci.* **2005**, *14*, 735–742; f) O. F. Lange, N.-A. Lakomek, C. Farès, G. F. Schröder, K. F. A. Walter, S. Becker, J. Meiler, H. Grubmüller, C. Griesinger, B. L. de Groot, *Science* **2008**, *320*, 1471–1475.
[7] a) L. E. Kay, J. H. Prestegard, *J. Am. Chem. Soc.* **1987**, *109*, 3829–3835; b) H. Sun, L. E. Kay, V. Tugarinov, *J. Phys. Chem. B* **2011**, *115*, 14878–14884.
[8] V. Tugarinov, R. Sprangers, L. E. Kay, *J. Am. Chem. Soc.* **2007**, *129*, 1743–1750.
[9] a) S.-H. Yang, A. Galanis, A. D. Sharrocks, *Mol. Cell. Biol.* **1999**, *19*, 4028–4038; b) C.-I. Chang, B.-e. Xu, R. Akella, M. H. Cobb, E. J. Goldsmith, *Mol. Cell* **2002**, *9*, 1241–1249.
[10] V. Tugarinov, L. E. Kay, *J. Am. Chem. Soc.* **2006**, *128*, 7299–7308.
[11] a) Á. Garai, A. Zeke, G. Gógl, I. Törő, F. Fördős, H. Blankenburg, T. Bárkai, J. Varga, A. Alexa, D. Emig, M. Albrecht, A. Reményi, *Sci. Signaling* **2012**, *5*, ra74; b) Y. Tokunaga, K. Takeuchi, H. Takahashi, I. Shimada, *Nat. Struct. Mol. Biol.* **2014**, *21*, 704–711.
[12] S. B. Patel, P. M. Cameron, B. Frantz-Wattley, E. O'Neill, J. W. Becker, G. Scapin, *Biochim. Biophys. Acta Proteins Proteomics* **2004**, *1696*, 67–73.
[13] M. S. Marlow, J. Dogan, K. K. Frederick, K. G. Valentine, A. J. Wand, *Nat. Chem. Biol.* **2010**, *6*, 352–358.
[14] a) E. J. Barreiro, A. E. Kümmerle, C. A. M. Fraga, *Chem. Rev.* **2011**, *111*, 5215–5246; b) C. S. Leung, S. S. F. Leung, J. Tirado-Rives, W. L. Jorgensen, *J. Med. Chem.* **2012**, *55*, 4489–4500.
[15] a) B. M. Baker, K. P. Murphy, *Biophys. J.* **1996**, *71*, 2049–2055; b) R. N. Goldberg, N. Kishore, R. M. Lennen, *J. Phys. Chem. Ref. Data* **2002**, *31*, 231–370.
[16] S. F. Martin, J. H. Clements, *Annu. Rev. Biochem.* **2013**, *82*, 267–293.

Received: August 2, 2016
Revised: September 21, 2016
Published online: October 20, 2016

